Electrochemical Characterization of Equilibria Involving Catalyst Precursors: Cyclic Voltammetry of Labile Organorhodium Complexes in Coordinating Solvents

Joseph Orsini and William E. Geiger*

Department of Chemistry, University of Vermont, Burlington, Vermont 05401

Received January 27, 1999

Cyclic voltammetry (CV) has been used to characterize equilibria between $[Rh(COD)_2]^+$ and $[Rh(COD)(solv)_2]^+$, where COD = cyclooctadiene and solv = acetone, 2-butanone, or acetonitrile. In donor solvents the reversible one-electron reduction of $[Rh(COD)_2]^{+/0}$ obeys the voltammetric diagnostics for a chemical reaction preceding electron transfer (a CE mechanism). The cathodic current for this wave is monitored as a function of CV scan rate in order to derive both equilibrium and rate constants for addition and elimination of COD from the metal center. The rate of addition of COD to $[Rh(COD)(solv)_2]^+$ is not significantly solvent-dependent, whereas elimination of COD from $[Rh(COD)_2]^+$ is about 4400 times faster for solv = CH_3CN than for either acetone or 2-butanone. The exchange reaction is apparently associative in both directions, following a $16e^-/18e^-$ pathway. Electrochemical methods are shown to provide a useful alternative to optical and magnetic resonance methods for the characterization of organometallic systems with labile ligands.

Introduction

Coordinatively unsaturated organometallic compounds are intermediates in a variety of stoichiometric and catalytic reactions.[1] Convenient precursors of these reactive intermediates sometimes have an easily displaced two-electron ligand such as a solvent molecule. Knowledge of the equilibrium thermodynamics and kinetics of solvent addition reactions (eq 1) and substitution reactions (eq 2) are important in defining the

$$L_nM + S \rightleftharpoons L_nM{-}S \quad (1)$$

$$L_nM + S \rightleftharpoons L_{n-1}M{-}S + L \quad (2)$$

possible role of metal solvates (L_nM−solv or $L_{n-1}M$−solv) and desolvates (L_nM) in a reaction scheme. Optical spectroscopy and NMR spectroscopy have been most commonly used[2] for the characterization of these systems, but in some cases the available methods are not suitable (e.g., lack of chromophores or resonating nuclei, a mismatch of the time scale of the spectroscopic tool with that of the equilibrating reaction, or the presence of paramagnetic species). The broad time domains of electrochemical techniques such as cyclic voltammetry (CV) make them useful for the characterization of reactions coupled to electron-transfer processes.[3a] In particular, slow voltammetry experiments may yield dynamic information on systems that are "frozen" on NMR or other spectroscopic time scales. Furthermore, it may be easier to detect a minor species by electrochemistry if it is the more easily electrolyzed species because of the perturbation of concentrations in the diffusion layer during the voltammetric scan. These methods have been grossly underutilized, however, for the characterization of labile organometallic complexes.[3b]

Standard approaches in organometallic electrochemistry favor the use of poorly coordinating solvents such as chloroalkanes or ethers in order to avoid situations such as that shown in eq 2.[4] The present paper shows that voltammetry is a potentially powerful technique for quantifying the metal complex/solvent equilibria that are central to the action of some important organometallic reactions in solvents of modest coordinating ability.

The solvent exchange with L_nM may be probed by voltammetry, provided that at least one species taking part in the equilibrium is electroactive (e.g., L_nM (eq 1 or eq 2), L_nM−solv (eq 1), or $L_{n-1}M$−solv (eq 2)). Then eq 1 (or eq 2) combines with eq 3 (where L_nM is assumed to be the reducible species) to describe a CE mechanism, i.e., one in which a chemical reaction (eq 1 or 2) precedes an electron transfer (eq 3).[5]

$$L_nM + e^- \rightleftharpoons \text{product(s)} \quad (3)$$

The kinetics of the equilibration may be probed if the time scale of the voltammetry (ca. $10-10^{-6}$ s) can be

(1) (a) Collman, J. P.; Hegedus, L. S.; Norton, J. R.; Finke, R. G. *Principles and Applications of Organotransition Metal Chemistry*; University Science Books, Mill Valley, CA, 1987; pp 524 ff. (b) Atwood, J. D. *Inorganic and Organometallic Reaction Mechanisms*; Brooks/Cole: Monterey, CA, 1985; Chapter 6.

(2) Jordan, R. B. *Reaction Mechanisms of Inorganic and Organometallic Systems*, 2nd ed.; Oxford University Press: New York, 1998; Chapter 9.

(3) (a) Bard, A. J.; Faulkner, L. R. *Electrochemical Methods*; Wiley: New York, 1980; p 435. (b) Amatore, C.; Azzabi, M.; Jutand, A. *J. Am. Chem. Soc.* **1991**, *113*, 1670.

(4) Geiger, W. E.; Hawley, M. D. In *Electrochemical Methods, Physical Methods of Chemistry*, 2nd ed.; Rossiter, B. W., Hamilton, J. F., Eds.; Wiley: New York, Vol. II, pp 27−29.

(5) (a) Nicholson, R. S.; Shain, I. *Anal. Chem.* **1964**, *36*, 706. (b) Reference 3a, pp 445−448. (c) Saveant, J.-M.; Vianello, E. *Electrochim. Acta* **1963**, *8*, 905 (d) Speiser, B. *J. Electroanal. Chem. Interfacial Electrochem.* **1991**, *301*, 15.

10.1021/om9900566 CCC: $18.00
Publication on Web 04/21/1999

adjusted to be comparable to the half-life of one reaction direction. It is not necessary to know the electrolysis product(s). One is simply using voltammetry as an analytical probe for the electroactive species; only the observed currents go into the quantitative calculations.[6]

Complexes of the general type [Rh(η^4-diolefin)L(solv)]$^+$ (L = solvent or group 13 ligand) are catalysts or catalyst precursors for a number of important processes such as asymmetric hydrogenations, the arylation of aldehydes, and olefin isomerizations. [7−14]

The activities of the Rh(I) complexes are markedly solvent-dependent,[7−9,13−16] implying that solvent addition and exchange equilibria (eqs 1 and 2) influence the effectiveness of the catalyst. We now report equilibrium and rate constants for solvento complexes formed when $[Rh(COD)_2]^+$ (COD = cyclooctadiene) is dissolved in three donor solvents (acetone, 2-butanone, and acetonitrile), showing the relevance of CV measurements to the characterization of labile organometallic complexes. The reduction of $[Rh(COD)_2]^+$ in (noncoordinating) chloroalkanes proceeds through a 17-electron radical which subsequently forms 16-electron Rh(η^4-COD)(η^3-C_8H_{13}).[17]

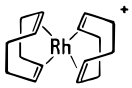

Experimental Section

Chemicals. All manipulations were performed under an atmosphere of dinitrogen using solvents distilled from drying agents. Electrochemical measurements were conducted in a Vacuum Atmospheres drybox. Solvents used for electrochemistry were of the highest quality commercially available (e.g., Burdick and Jackson or Aldrich "gold label") and further purified by vacuum distillation from molecular sieves (acetone, 2-butanone, CH_3CN) or CaH_2 (CH_2Cl_2). $[NBu_4][PF_6]$ used as supporting electrolyte was prepared by metathesis of $[NH_4][PF_6]$ and $[NBu_4]I$ in acetone, recrystallized three times from 95% ethanol, and vacuum-dried at 373 K. $[Cp_2Co][PF_6]$ and ferrocene were purchased from Strem Chemical Co. and purified, the former by recrystallization from acetone/diethyl ether and the latter by sublimation.

$Ag[PF_6]$ and $Ag[BF_4]$ were used as received. Cyclooctadiene (Aldrich) was passed through alumina. $[Rh(COD)_2][PF_6]$, prepared by the method of Schrock and Osborne[7] from $[Rh(COD)Cl]_2$ and $Ag[PF_6]$ in the presence of COD, was recrystallized from CH_2Cl_2/diethyl ether and characterized by elemental analysis and ^{1}H NMR spectroscopy. $[Rh(COD)(acetone)_2]^+$ was generated by treatment of $[Rh(COD)Cl]_2$ with Ag salts in acetone[18] and studied in situ by voltammetry and NMR spectroscopy.

Electrochemistry. Voltammetric experiments were performed with a Princeton Applied Research Corp (PARC) Model 173 potentiostat with Model 175 Universal Programmer and Model 176 *i*/*E* converter and recorded on fast-response X−Y recorders or a Nicolet Model 4094A digital oscilloscope. A conventional three-electrode cell design was used, the experimental reference electrode being either an aqueous saturated calomel electrode (SCE) or (at temperatures below 273 K) a AgCl-coated silver wire. Potentials in this paper are referenced, however, to the ferrocene/ferrocenium couple as recommended by IUPAC.[19] The measured potentials for ferrocene (vs SCE) under our conditions were 0.48 V in acetone, 0.46 V in CH_2Cl_2, and 0.40 V in acetonitrile (all containing 0.1 M $[NBu_4][PF_6]$). Resistive losses were minimized through use of a Luggin probe[20] and positive-feedback *iR* compensation. The working electrode was a Pt disk (Bioanalytical Systems) with an electrochemically determined area[21] of 0.027 cm^2. It was polished with diamond pastes of diameters down to 0.25 μm, rinsed with Nanopure water, and vacuum-dried. Computer simulations of CV scans initially performed using a program based on the finite difference method of Feldberg[22] were later supplemented by computations with DIGISIM (Bioanalytical Systems).[23]

NMR Spectroscopy. Proton NMR spectra were recorded on a 250 MHz Bruker instrument using TMS as the chemical shift standard. For quantitative studies deuterated acetone (Aldrich) dried over molecular sieves was vacuum-distilled into an NMR tube containing, typically, 6.22 mg of $[Rh(COD)_2][PF_6]$ and 2.64 mg of $[Cp_2Co][PF_6]$. The latter served as an internal standard. The tube was sealed under vacuum, after which the solution level was marked on the tube for later volume calibration. NMR spectra were collected with a 2 s delay. Integrations of the resonances were found to have relative standard deviations of 15%.

Results

Requirements for Application of Voltammetric Theory to Metal/Solvent Equilibria. Successful application of the theory of CE mechanisms to quantification of both the kinetics and thermodynamics of solvent replacement reactions requires that (1) at least one metal-containing species is electroactive, (2) the fast experiment (or "frozen equilibrium") limit be achievable at higher scan rates, ν, from which an equilibrium constant may be derived, and (3) an intermediate scan rate regime be achievable in which the measured current responses have a contribution from the rate of interconversion of the metal complex and its solvate. An alternative to (2) is possible if there is a way of forcing the equilibrium to one side, e.g., by pH adjustments or ligand additions that may suppress the solvent complex formation. The system $[Rh(COD)_2]^+$ in donor solvents is one in which such an adjustment can be made by addition of excess COD to solutions of the complex.

(6) (a) Saveant, J.-M.; Xu, F. *J. Electroanal. Chem. Interfacial Electrochem.* **1986**, *208*, 197. (b) Hertl, P.; Speiser, B. *J. Electroanal. Chem. Interfacial Electrochem.* **1988**, *250*, 237.

(7) (a) Schrock, R. R.; Osborn, J. A. *J. Am. Chem. Soc.* **1971**, *93*, 2397. (b) Shapley, J. R.; Schrock, R. R.; Osborn, J. A. *J. Am. Chem. Soc.* **1969**, *91*, 2816. (c) Schrock, R. R.; Osborn, J. A. *J. Chem. Soc., Chem. Commun.* **1970**, 567.

(8) Anderson, M. P.; Pignolet, L. H. *Inorg. Chem.* **1981**, *20*, 4101.

(9) Oi, S.; Moro, M.; Inoue, Y. *Chem. Commun.* **1997**, 1621.

(10) Zhu, G.; Cao, P.; Jiang, Q.; Zhang, X. *J. Am. Chem. Soc.* **1997**, *119*, 1799.

(11) Burk, M. J.; Feaster, J. E. *J. Am. Chem. Soc.* **1992**, *114*, 6266.

(12) RajanBabu, T. V.; Ayers, T. A.; Casalnuovo, A. L. *J. Am. Chem. Soc.* **1994**, *116*, 4101.

(13) Zhou, Z.; Facey, G.; James, B. R.; Alper, H. *Organometallics* **1996**, *15*, 2496.

(14) Noyori, R. *Asymmetric Catalysis in Organic Synthesis*; Wiley: New York, 1994.

(15) Denise, B.; Pannetier, G. *J. Organomet. Chem.* **1978**, *161*, 171.

(16) Howarth, O. W.; McAteer, C. H.; Moore, P.; Morris, G. E. *J. Chem. Soc., Dalton Trans.* **1981**, 1481.

(17) Orsini, J.; Geiger, W. E. *J. Electroanal. Chem.* **1995**, *380*, 83.

(18) Schrock, R. R.; Osborn, J. A. *J. Am. Chem. Soc.* **1971**, *93*, 3089.

(19) Gritzner, G.; Kuta, J. *Pure Appl. Chem.* **1984**, *56*, 461.

(20) (a) Rieger, P. H. *Electrochemistry*, 2nd ed.; Chapman and Hall: New York, 1994; p 168. (b) Sawyer, D. T.; Sobkowiak, A.; Roberts, J. L., Jr. *Electrochemistry for Chemists*; Wiley: New York, 1995; p 250.

(21) Adams, R. N. *Electrochemistry at Solid Electrodes*; Marcel Dekker: New York, 1969; p 124.

(22) Feldberg, S. W. In *Electroanalytical Chemistry*; Bard, A. J., Ed.; Marcel Dekker: New York, 1969; Vol. 3, p 199.

(23) Rudolph, M.; Reddy, D. P.; Feldberg, S. W. *Anal. Chem.* **1994**, *66*, 589A.

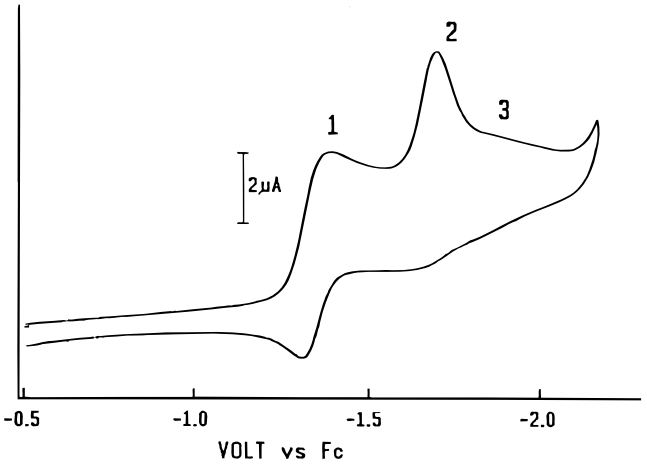

Figure 1. CV scan of formally 1.1 mM $[Rh(COD)_2]^+$ in acetone/0.1 M $[NBu_4][PF_6]$ at a Pt disk, $T = 298$ K, $\nu = 0.2$ V s^{-1}.

Figure 1shows a scan of ca. 1 mM $[Rh(COD)_2]^+$ in acetone at $\nu = 0.2$ V/s. The two main cathodic peaks (labeled 1 and 2) come at approximately the same potentials as the two one-electron reductions ascribed to the Rh(I)/Rh(0) and Rh(0)/Rh(−I) couples in CH_2Cl_2 and are assigned to the same redox processes (eqs 4 and 5).[17] The current levels are, however, less than those

$$[Rh(COD)_2]^+ + e^- \rightleftharpoons Rh(COD)_2 \quad (4)$$

$$Rh(COD)_2 + e^- \rightleftharpoons [Rh(COD)_2]^- \quad (5)$$

observed for comparable organometallic complexes at similar concentrations at this electrode. When COD is added to the solution, the currents for waves 1 and 2 increase, both waves become fully reversible, and feature 3 disappears (see the figure in the Supporting Information). These changes constitute evidence for exchange between acetone and one COD ligand (eq 6).

$$[Rh(COD)(acetone)_2]^+ + COD \underset{k'_b}{\overset{k'_f}{\rightleftharpoons}} [Rh(COD)_2]^+ + acetone \quad (6)$$

CV Diagnostics for CE Mechanisms of Labile Complexes: General Considerations. The general theory for a chemical reaction preceding electron transfer depends on a variety of factors involving both the relative and absolute values of the quantities k'_f and k'_b, compared to the voltammetric observation time t (=(scan range in V)/(scan rate ν)).[5,6] The most important diagnostics involve how up to four measurables[24] change with ν, namely (i) the current function $X = i_p/\nu^{1/2}$ [25] and, for a chemically reversible couple (e.g., L_nM/L_nM^- in eq 2), (ii) the ratio of reverse to forward currents (i_a/i_c for a reduction), (iii) the apparent formal potential $E_{1/2}$ (measured as the average of the cathodic and anodic peak potentials $E_{p,c}$ and $E_{p,a}$, respectively), and (iv) the separation ΔE_p (=$E_{p,a} - E_{p,c}$). We will discuss each of these for the Rh−COD systems under study. The true (i.e., thermodynamic) and apparent $E_{1/2}$ potentials of $[Rh(COD)_2]^+$ in different media are collected in Table 1.

Table 1. Apparent and Thermodynamic Formal Potentials of the $[Rh(COD)_2]^+/Rh(COD)_2$ Couple in Various Solvents[a]

medium	$E_{1/2}$(app) ($\nu = 0.2$ V/s)	$E_{1/2}$
acetone	−1.340	−1.310
2-butanone	−1.330	−1.300
CH_2Cl_2	−1.322	−1.322
CH_2Cl_2/CH_3CN[b]	−1.357	−1.359
CH_3CN[c]	$E_{pc} = -2.22$[d]	

[a] Conditions: Potentials in V vs ferrocene/ferrocenium, supporting electrolyte 0.1 M $[NBu_4][PF_6]$, ambient temperatures. $E_{1/2}$ was calculated from the average of $E_{p,c}$ and $E_{p,a}$. [b] $[CH_3CN] = 0.012$ M. [c] COD added, concentration 0.50 M. [d] Irreversible cathodic wave ascribed to $[Rh(COD)(CH_3CN)_2]^+$.

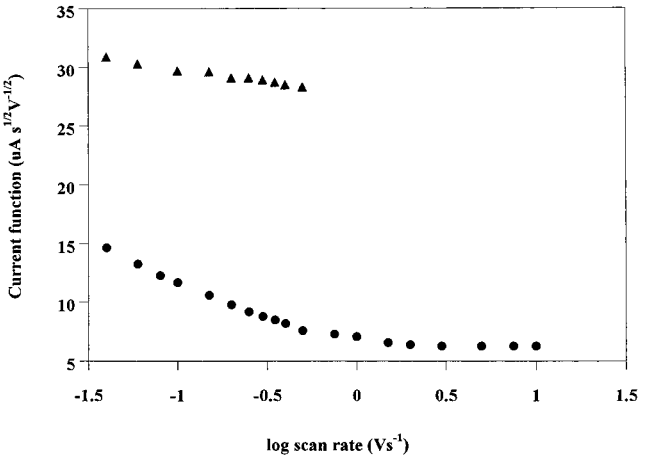

Figure 2. Current function, X (=$i_p/\nu^{1/2}$), at different scan rates for 1.1 mM $[Rh(COD)_2]^+$ in acetone/0.1 M $[NBu_4][PF_6]$ at 298 K: (●) no added COD; (▲) 17 mM added COD.

Pragmatically, however, it is the morphology of the CV wave that is commonly the first indicator of a "preceding reaction" scenario. In Figure 1, peak 1 does not have the normal "diffusional" tail; instead it is approximately plateau-shaped, indicative that the system is in an intermediate time scale regime in which the kinetics of the equilibration are affecting the amount of reducible substance ($[Rh(COD)_2]^+$) at the electrode surface. Considerably higher or lower scan rates both yield more normal peak shapes. The broad minor feature 3 in Figure 1 appears to arise from a solvento complex and becomes prominent at larger ν. Only the currents for wave 1 are required in the analysis.

CV Diagnostics Applied to $[Rh(COD)_2]^+$ in Acetone. Application of diagnostics i−iv shows that the rate of the diolefin association reaction (k'_f in eq 6) partially governs the quantity of $[Rh(COD)_2]^+$ available for reduction in wave 1: over a wide *increase* in scan rates (i) the current function X *drops* by more than half (circles in Figure 2), (ii) the ratio i_a/i_c goes through a maximum (circles in Figure 3),[26] (iii) $E_{1/2}$ *increases* until

(24) Geiger, W. E. In *Laboratory Techniques in Electroanalytical Chemistry*, 2nd ed.; Kissinger, P. T., Heineman, W. R., Eds.; Marcel Dekker: New York, 1996; Chapter 23.

(25) Definitions of symbols: X (=$i_p/\nu^{1/2}$) is the current function; i_p = CV peak current; $E_{p,c}$ (or $E_{p,a}$) = CV cathodic (or anodic) peak potential; $\Delta E_p = |E_{p,a} - E_{p,c}|$; i_a/i_c = ratio of anodic to cathodic currents measured by the method of Nicholson (Nicholson, R. S. *Anal. Chem.* **1965**, *37*, 1351).

(26) The ratio of reverse to forward currents, i_a/i_c in the case of a reduction, normally may be equal to or greater than unity for a CE mechanism. The slow reaction of $Rh(COD)_2$ *following* reduction, and forming $Rh(COD)(C_8H_{13})$, is responsible for i_a/i_c falling below unity at low scan rates.

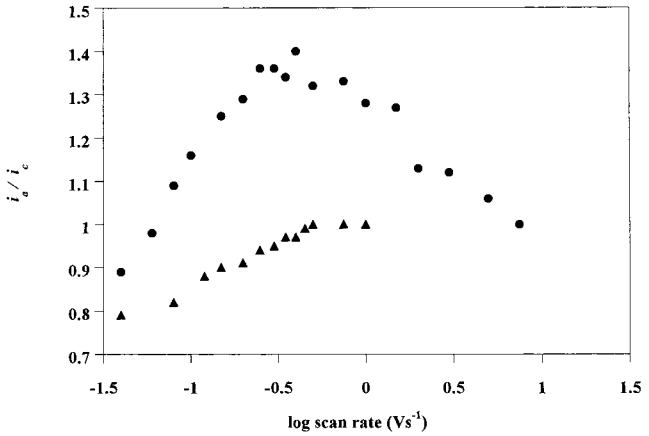

Figure 3. Ratio of reverse-to-forward currents for first reduction wave of formally 1.1 mM $[Rh(COD)_2]^+$ in acetone/0.1 M $[NBu_4][PF_6]$ at different scan rates (T = 299 K): (●) no added COD; (▲) 17 mM added COD.

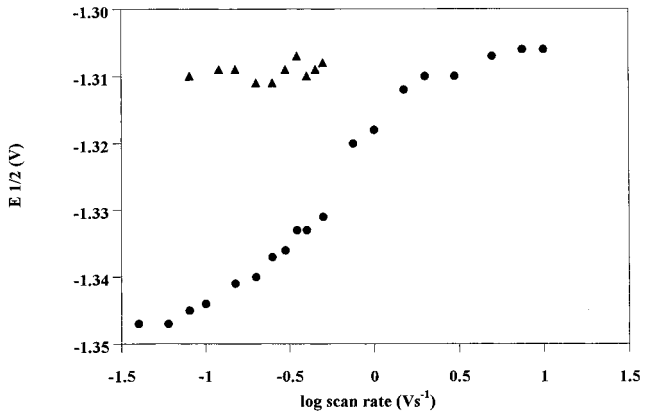

Figure 4. Apparent $E_{1/2}$ values (vs ferrocene) measured for $[Rh(COD)_2]^+$ in acetone at different scan rates (T = 299 K; formal concentration 1.1 mM): (●) no added COD; (▲) 17 mM added COD.

it reaches a constant value (circles in Figure 4), and (iv) ΔE_p *decreases*. All four trends are as predicted for a CE mechanism.[6,26]

Measurement of the Thermodynamic Equilibrium Constant, K_{assoc}, in Acetone. The value of the current function in the fast scan limit, X_{lim} (see Figure 2), is less than one-fourth that observed (X_o) when excess COD is used to push the equilibrium of eq 6 to the right (6.3 vs 28.9 μA $s^{1/2}$ $V^{-1/2}$); these current functions converted to mole fractions of Rh-containing species were used to calculate an equilibrium constant. Five replicates in separate experiments gave K_{assoc} = 300 (±27) M^{-1} for eq 7.[27]

$$K_{assoc} = [Rh(COD)_2{}^+]/[Rh(COD)(acetone)_2{}^+][COD] \quad (7)$$

A similar approach was used at several temperatures between 240 and 300 K, resulting in a linear plot of ln K_{assoc} vs $1/T$ (Figure 5) and the values $\Delta H°$ = −1.8 kcal/mol and $\Delta S°$ = 5.2 cal mol^{-1} K^{-1}. As the temperature was lowered, the scan rate required to reach the fast scan limit X_{lim} decreased (Figure 6). The value of X_o to be compared with X_{lim} was calculated from the value at 300 K (28.9 μA $s^{1/2}$ $V^{-1/2}$, vide supra) corrected for the lower diffusion coefficient expected for $[Rh(COD)_2]^+$ at lower temperatures. This correction was approximated by measuring the temperature dependence of the diffusion coefficient, D_o, of the cobaltocenium ion in acetone by chronoamperometry over the same temperature range. A plot of D_o vs T was linear with a slope of 1.34 × 10^{-7} cm^2 s^{-1} deg^{-1}, and this correction was applied to the values of X_o expected for $Rh(COD)_2^+$ at different temperatures.[28]

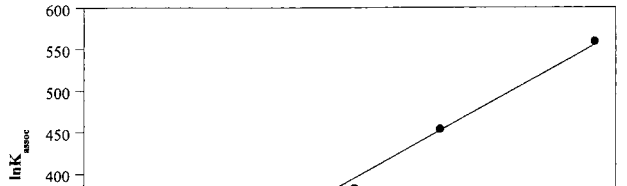

Figure 5. van't Hoff plot of association constant defined by eq 7 for $[Rh(COD)_2]^+$ in acetone (correlation coefficient 0.998).

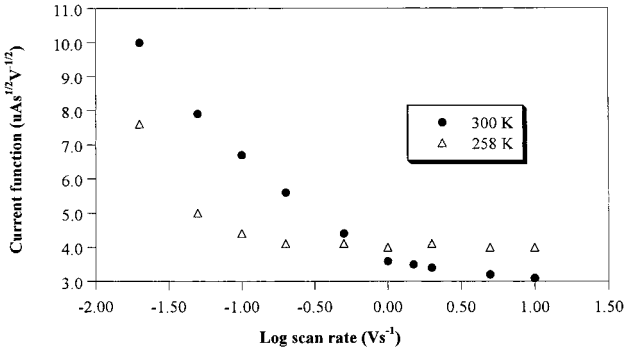

Figure 6. Comparative current functions for 1.0 mM $[Rh(COD)_2]^+$ in acetone at two different temperatures: (●) 300 K; (△) 258 K.

K_{assoc} was also measured at room temperature by ^1H NMR spectroscopy of $Rh[(COD)_2]^+$ in d_6-acetone to which a known amount of $[Cp_2Co][PF_6]$ was added as an internal standard. In four replicate experiments a value of 321 (±55) M^{-1} was obtained, in good agreement with the value obtained through voltammetry.

Measurement of the Rate Constants in Acetone. Once K_{assoc} is known, the rates of the association (k'_f of eq 6) and dissociation (k'_b) of COD may be obtained from the X vs v data (e.g. Figure 2) in the intermediate kinetic regime (v < 1.5 V/s at ambient temperatures). Although digital simulations will generally give the most quantitative results, good estimates of the rates can be obtained using working curves presented by Saveant and Xu.[6] In the Appendix, the pertinent calculations are presented in which $i_p/i_p°$ is plotted as a

(27) If a solvent takes part in a chemical reaction, the relationship between the equilibrium constant derived for that reaction from a kinetic model, K_{eq}(kin), and that derived from the law of mass action, K_{eq}(thermo), is K_{eq}(kin) = K_{eq}(thermo)[solv]^{ro}, where [solv] is the nominal concentration of the solvent and "ro" is its reaction order. If the reaction order is unknown, the solvent is omitted from the expression and K_{eq}(kin) = K_{eq}(thermo); see: Levine, I. N. *Physical Chemistry*, 4th ed.; McGraw-Hill: New York, 1995; pp 508−510.

(28) The following diffusion coefficients were measured at 298 K by chronoamperometry in acetone/0.1 M $[NBu_4][PF_6]$: $[Cp_2Co][PF_6]$, 1.62 × 10^{-5} cm^2 s^{-1}; $[Rh(COD)_2][PF_6]$, 1.77 × 10^{-5} cm^2 s^{-1}.

Table 2. Equilibrium and Rate Constants for Solvent-Involved Equilibria of $[Rh(COD)_2]^+$.

medium	K_{assoc}[a]	K_{kin}[b]	k'_b[c] (s^{-1})	k_b[d] (M^{-1} s^{-1})	k_f[e] (M^{-1} s^{-1})
acetone	300 M^{-1}	4.06×10^3	7.3	0.54	2.40×10^3
2-butanone	370 M^{-1}	4.37×10^3	6.0	0.51	2.44×10^3
0.023 M CH_3CN[f]	9.6×10^{-3} M	9.6×10^{-3} M	49.7	2.73×10^3	1.05×10^3

[a] $K_{assoc} = [Rh(COD)_2^+]/[Rh(COD)(solvent)^+][COD]$ (eq 7). [b] $K_{kin} = K_{assoc}[solv]$ when reaction is conducted in virtually pure solvent, $= k'_f/k'_b$ (eq 6). [c] From eq 6. [d] $k_b = k'_b/[solvent]$. [e] From eq 6. [f] In CH_2Cl_2.

function of $\log [(\lambda_D)^{1/2} K_{assoc} X_o]$, where i_p is the measured peak current at a given scan rate, $i_p°$ is that expected in the absence of any dissociation (i.e., all $[Rh(COD)_2]^+$, computed from the current function in the presence of excess COD), X_o is the formal concentration of the rhodium complex (1.09×10^{-3} M for the scan in Figure 1), and λ_D is a dimensionless kinetic parameter defined as

$$\lambda_D = (RT/F)(k'_b/v) \quad (8)$$

where $RT/F = 0.0257$ V at 298 K. Using data points at $v = 0.2$, 0.75, and 1.0 V/s, a value of $k'_b = 7.38$ s^{-1} was obtained. The associative rate k'_f is then calculated from k'_b and K_{assoc} ($= k'_f/k'_b$). The resulting values are collected in Table 2.

Theoretical Simulations of CV Responses. As a check on the approach of using current functions and graphical methods to derive thermodynamic and kinetic parameters, digital simulations were undertaken for the CV responses of $[Rh(COD)_2]^+$ in acetone. This approach has the added benefit of interrogating the entire morphology of the CV curve rather than relying on a single-point (i.e., peak current) measurement. Limited calculations were originally performed by the finite difference method of Feldberg,[22] and subsequently a more complete set was obtained using the fast implicit finite difference method.[23] The two approaches gave identical results and reproduced the experimental wave shapes (e.g., Figure 7). When the values for K_{assoc} and k'_b obtained from graphical procedures (vide supra and Table 2) were used in simulations, the calculated and observed current functions were in reasonable agreement over more than 2 orders of magnitude change in scan rate (Figure 8).

These simulations also revealed that the 17-electron radical $Rh(COD)_2$ undergoes a slow reaction following its formation from the Rh(I) starting material. A first-order rate constant of $k_c = 0.16$ s^{-1} accounts for the fact that i_a/i_c ratios fall below unity (Figure 3) at very slow scan rates. Overall, then, the mechanism for the *first* reduction wave of $[Rh(COD)_2]^+$ in acetone (wave 1 in Figure 1) is the CEC process of eqs 6 followed by eqs 4 and 9.

$$[Rh(COD)(acetone)_2]^+ + COD \underset{k'_b}{\overset{k'_f}{\rightleftharpoons}} [Rh(COD)_2]^+ + acetone \quad (C) \quad (6)$$

$$[Rh(COD)_2]^+ + e^- \rightleftharpoons Rh(COD)_2 \quad (E) \quad (4)$$

$$Rh(COD)_2 \xrightarrow{k_c} \text{unconfirmed product(s)} \quad (C) \quad (9)$$

Behavior of $[Rh(COD)_2]^+$ in 2-Butanone. Befitting the similarity between acetone and 2-butanone, very similar electrochemical responses were observed when $[Rh(COD)_2]^+$ was investigated in the latter. The expected diagnostics were seen for i_a/i_c, $E_{1/2}$ (Table 1), and ΔE_p. The current function X decreased from 6.25 μA $s^{1/2}$ $V^{-1/2}$ at $v = 0.05$ V s^{-1} to 2.93 μA $s^{1/2}$ $V^{-1/2}$ at $v > 1$ V s^{-1}. With 10-fold excess COD, X in the fast scan limit (X_o) was 14.2. Equilibrium and rate constants calculated by the procedures given above gave the values in Table 2, which are quite close to those found for acetone media.

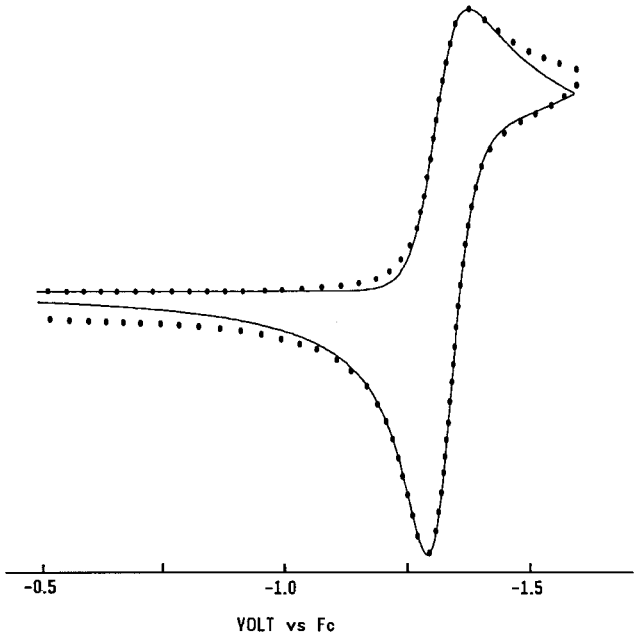

Figure 7. Comparison of experimental (dots) and theoretical (solid line) CV curves for $[Rh(COD)_2]^+$ in acetone (scan rate 0.3 V s^{-1}, $T = 299$ K): theoretical calculation by DIGISIM based on CEC mechanism of eqs 6, 4, and 9, with $K_{assoc} = 300$ M^{-1}, $k'_b = 7.3$ s^{-1}, $E_{1/2} = -1.31$ V, $k_s = 0.1$ cm s^{-1}, $\alpha = 0.5$, and $k_c = 0.16$ s^{-1}.

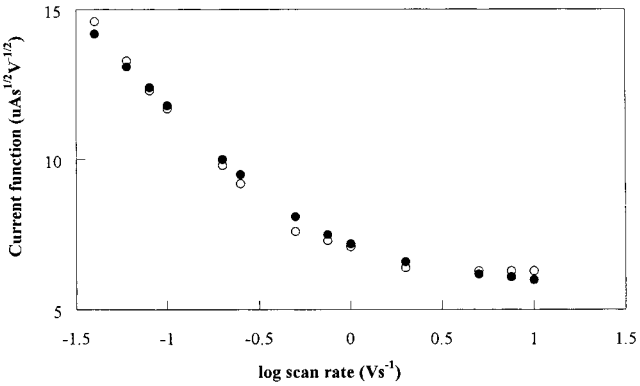

Figure 8. Comparison of experimental (●) and calculated (○) cathodic peak currents for wave 1 in Figure 1 (1.1 mM $[Rh(COD)_2]^+$ in acetone/0.1 M $[NBu_4][PF_6]$) at different scan rates. Theoretical values were taken from calculations employing parameters in the caption of Figure 7.

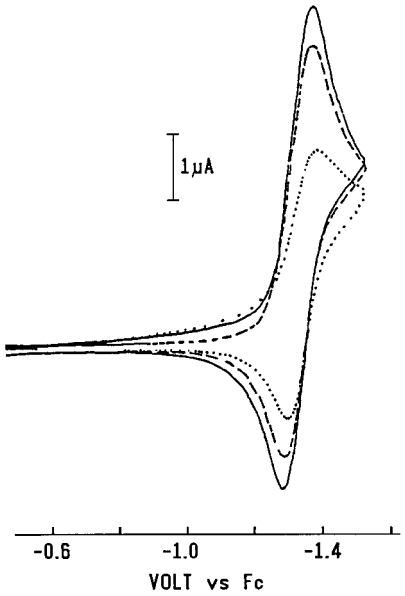

Figure 9. CV scans (300 K, 0.2 V s^{-1}) of formally 0.95 mM $[Rh(COD)_2]^+$ in CH_2Cl_2/0.1 M $[NBu_4][PF_6]$ with increasing amounts of CH_3CN added: (solid line) pure CH_2Cl_2; (dashed line) 1.8 mM CH_3CN; (dotted line) 7.0 mM CH_3CN.

Table 3. Voltammetric Parameters for the $[Rh(COD)_2]^+/Rh(COD)_2$ Couple in CH_2Cl_2/0.1 M $[NBu_4][PF_6]$ Containing Different Concentrations of CH_3CN[a].

$[CH_3CN]$ (mM)	X (μA $V^{-1/2}$ $s^{1/2}$)	$E_{1/2}$(app) (V)	ΔE_p (mV)
0	11.10	−1.322	80
1.8	9.46	−1.320	82
7.0	5.86	−1.341	88
11.6	3.50	−1.357	109

[a] Formal concentration of $[Rh(COD)_2]^+$ 0.95 mM, $\nu = 0.2$ V s^{-1}.

Behavior of $[Rh(COD)_2]^+$ in Acetonitrile. The stronger donor ligand CH_3CN forms isolable $[Rh(COD)(CH_3CN)_2]^+$ when reacted with $[Rh(COD)_2]^+$.[7,9,15] In fact, a formal 0.5 mM solution of $[Rh(COD)_2]^+$ in acetonitrile has no detectable wave near the potential expected for the bis-COD complex (ca. −1.3 V), even in the presence of a 100-fold excess of COD. Instead, there is a broad irreversible wave at $E_{p,c} = -2.22$ V, which we ascribe to the reduction of $[Rh(COD)(CH_3CN)_2]^+$. To study the equilibrium between $[Rh(COD)_2]^+$ and $[Rh(COD)(CH_3CN)_2]^+$, conditions were employed in which there was a more reasonable balance between the two sides of eq 10, namely dilute concentrations of CH_3CN (in

$$[Rh(COD)(CH_3CN)_2]^+ + COD \underset{k'_b}{\overset{k'_f}{\rightleftharpoons}} Rh[(COD)_2]^+ + 2CH_3CN \quad (10)$$

CH_2Cl_2) and an excess of COD. The sensitivity of the current levels for $[Rh(COD)_2]^+$ to the presence of CH_3CN is demonstrated in Figure 9, where addition of small amounts of CH_3CN to CH_2Cl_2 results in lowering of the peak current for $[Rh(COD)_2]^+$ (Table 3) and onset of the characteristic nondiffusional tail of the current past the switching potential (dotted-line curve of Figure 9).

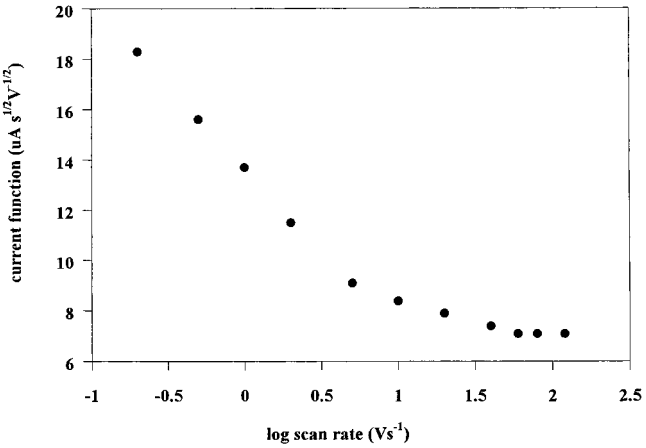

Figure 10. Current function (X) at different scan rates for formally 1.46 mM $[Rh(COD)_2]^+$ in CH_2Cl_2/0.1 M $[NBu_4][PF_6]$ containing 17 mM added COD and 37 mM added CH_3CN ($T = 299$ K).

Owing to the higher rate of solvent addition (k'_b in eq 10), higher scan rates were required to reach the fast scan limit in this medium compared to acetone. Figure 10 shows typical values of the resistance-corrected[29] current function, which reaches a constant value above about $\nu = 60$ V s^{-1}. A constant value of $X_o = 26.5$ μA $V^{-1/2}$ $s^{1/2}$ was found for pure CH_2Cl_2 solutions of $[Rh(COD)_2]^+$, allowing the calculation of K_{assoc} in eq 10. Four replicates using CH_3CN in 18−32-fold excess of $[Rh(COD)_2]^+$ gave $K_{assoc} = [9.6\ (\pm 0.5)] \times 10^{-3}$ M (Table 2). A graphical evaluation of the rate constants from the value of X at $\nu = 0.2$ V s^{-1} gave $k'_b = 49.7$ s^{-1} and k_b ($= k'_b/[CH_3CN]$) $= 2.39 \times 10^3$ M^{-1} s^{-1}, assuming a first-order dependence of k_b on $[CH_3CN]$. This process was repeated at different scan rates and concentrations of $[Rh(COD)_2]^+$, COD, and CH_3CN, with the results tabulated in Table 4. The average value of k_b was $[2.73\ (\pm 0.24)] \times 10^3$ M^{-1} s^{-1} (Table 2).

Discussion

The general solvent-for-COD exchange reaction may be written as eq 11, where solv = solvent. Comparison

$$[Rh(COD)(solv)_2]^+ + COD \underset{k'_b}{\overset{k'_f}{\rightleftharpoons}} [Rh(COD)_2]^+ + 2solv \quad (11)$$

of the rates k_f (for the *addition* of COD) is straightforward, since $k_f = k'_f/[COD]$ for all three solvents. Values of k_f between 1.1 and 2.4 M^{-1} s^{-1} are indicated (Table 2), demonstrating that the forward reaction of eq 11 is affected very little by changes in solvent, at least with the limited number of solvents we have investigated.

(29) Significant ohmic effects were in evidence even with use of positive feedback (see: Roe, D. K. In ref 24, Chapter 7) when scan rates above about 5 V s^{-1} were employed. We corrected the observed cathodic peak currents for ohmic loss with the help of the fact that X is inversely proportional to ΔE_p under the conditions of high ohmic loss ($\Delta E_p = 150-500$ mV) encountered under our conditions. Measurements made on 2 mM ferrocene in CH_2Cl_2/0.1 M $[NBu_4][PF_6]$ between 5 and 160 V s^{-1} confirmed this relationship with a correlation coefficient of 0.999. Corrections were made to X of the $[Rh(COD)_2]^{+/0}$ wave with the help of an internal standard of ferrocene, which gave the same peak current as the rhodium system. A similar correction procedure has been described elsewhere: Garcia, E.; Kwak, J.; Bard, A. J. *Inorg. Chem.* **1988**, *27*, 4377.

Table 4. Summary of Kinetic Data for Equilibration of $[Rh(COD)_2]^+$ with CH_3CN in CH_2Cl_2[a]

formal $[Rh(COD)_2]^+$	[COD]	$[CH_3CN]$	ν (V s^{-1})[b]	k'_b (s^{-1})[c]	$10^{-3}k_b$ (M^{-1} s^{-1})[d]
1.00	27	26	1.0	77	2.98
1.00	27	26	0.5	78	3.00
0.99	47	39	1.0	72	2.8
1.46	17	21	0.2	50	2.39
1.46	17	21	1.0	55	2.64
1.46	27	43	1.0	103	2.39
1.46	27	43	5.0	124	2.88

[a] Concentrations in mM, ambient temperatures. [b] Scan rate at which calculation of k'_b was performed. [c] As defined in eq 10. [d] $k_b = k'_b/[CH_3CN]$.

We hypothesize that the rate-determining step in the addition of COD to the 16-electron complex $[Rh(COD)(solv)_2]^+$ is associative, with an 18-electron complex (**A**) having a η^2-coordinated COD ligand being the most likely transition-state structure.

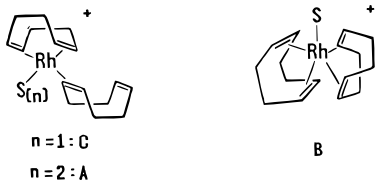

To compare the rates of the reverse reaction, that involving *elimination* of one COD by solvent, we note that $k_b = k'_b/[solv]$ and that we assume a reaction order of 1 in solv. Since data for acetone and 2-butanone were carried out in "pure" solvent, this assumption is unproven; it is reasonable, however, since a reaction order higher than unity for solv would imply the participation of termolecular processes. Under this assumption the elimination of COD is seen to be about 4400 times faster in CH_3CN than in the two ketonic solvents (k_b values in Table 2). This fact argues for a transition-state structure involving a coordinated solvent and two η^4-bound COD ligands (**B**), an 18-electron system. We cannot, however, rule out a 16-electron structure such as **C**, which could occur if the attack of solv and a η^4 to η^2 reorganization of one COD ligand were simultaneous, in an S_N2-like process. This latter mechanism has been proposed for the replacement of COD by norbornadiene for coordinatively *saturated* complexes such as CpCo(η^4-COD) in donor solvents such as CH_3CN.[30]

The present results on exchange of COD with solvent molecules between $[Rh(COD)L]^+$ (L = COD or solvent) suggests that the reactions are associative in both directions.

Finally, we note that the use of electrochemistry to characterize labile organometallics may be pursued under an attractive range of conditions and rate constants if one considers that voltammetry may be quantitatively conducted at quite low temperatures[31] or over a time scale regime of at least a 10^6-fold change using microelectrodes,[32] in relatively nonpolar solvents,[33] and even in the absence of supporting electrolytes.[33b,34] We encourage the organometallic community to consider these approaches for the characterization of relevant catalyst systems.

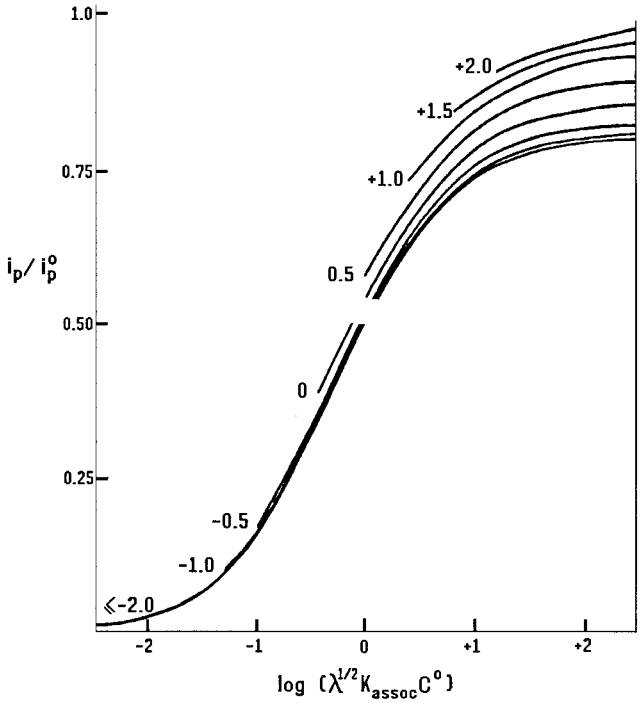

Figure 11.

Appendix

The following procedure was used to estimate the value of the rate constant for the dissociation of COD, k'_b in eq 6, from experimental data at $\nu = 0.2$ V s^{-1} on an acetone solution having a formal concentration of 1.09 mM, combined with working curves of i_p/i_p° vs $\log(\lambda^{1/2}K_{assoc}X_o)$ provided in ref 6a. Definitions are as follows: i_p is the cathodic peak current for the first reduction wave of $[Rh(COD)_2]^+$ at scan rate ν; i_p° is the current which would be expected in the absence of any dissociation reaction (i.e., for 1.09 mM $[Rh(COD)_2]^+$); $\lambda = (RT/F)k'_b/n$ (where $RT/F = 0.0257$ V at 298 K); X_o is the formal concentration of the electroactive species.

The value of i_p° is obtained from a scan of $[Rh(COD)_2]^+$ in the presence of excess COD; if such an experimental condition is not available, the value of i_p° may be estimated from currents measured for analogous complexes with expected similar diffusion coefficients. In the present case $i_p/i_p^\circ = 0.34$. The family of

(30) Wakatsuki, Y.; Yamazaki, H.; Kobayashi, T.; Sugawara, Y. *Organometallics* **1987**, *6*, 1191.

(31) (a) Bowyer, W. J.; Engelman, E. E.; Evans, D. H. *J. Electroanal. Chem. Interfacial Electrochem.* **1989**, *262*, 67. (b) Evans, D. H.; Lerke, S. A. In Reference 24, Chapter 16. (c) Baer, C. D.; Camaioni-Neto, C. A.; Sweigart, D. A.; Bond, A. M.; Mann, T. F.; Tondreau, G. A. *Coord. Chem. Rev.* **1989**, *93*, 1. (d) Dalton, E. F.; Ching, S.; Murray, R. W. *Inorg. Chem.* **1991**, *30*, 2642. (e) Green, S. J.; Rosseinsky, D. R.; Toohey, M. J. *J. Chem. Soc., Chem. Commun.* **1994,** 325.

(32) Theory for a CE mechanism at ultramicroelectrodes: (a) Fleischman, M.; Pons, S. *J. Electroanal. Chem. Interfacial Electrochem.* **1988**, *250*, 285. (b) Oldham, K. B. *J. Electroanal. Chem. Interfacial Electrochem.* **1991**, *313*, 3.

(33) (a) Zoski, C. G.; Sweigart, D. A.; Stone, N. J.; Rieger, P. H.; Mocellin, E.; Mann, T. F.; Mann, D. R.; Gosser, D. K.; Doeff, M. M.; Bond, A. M. *J. Am. Chem. Soc.* **1988**, *110*, 2109. (b) Cooper, J. B.; Bond, A. M. *J. Electroanal. Chem. Interfacial Electrochem.* **1991**, *315*, 143. (c) Tsionsky, M.; Bard, A. J.; Mirkin, M. V. *J. Am. Chem. Soc.* **1997**, *119*, 10785.

(34) (a) Drew, S. M.; Wightman, R. M.; Amatore, C. A. *J. Electroanal. Chem. Interfacial Electrochem.* **1991**, *317*, 117. (b) Oldham, K. B. *J. Electroanal. Chem. Interfacial Electrochem.* **1992**, *337*, 91. (c) Oldham, K. B.; Cardwell, T. J.; Santos, J. H.; Bond, A. M. *J. Electroanal. Chem.* **1997**, *430*, 25, 39.

working curves in the Figure 11 differ in their values of $\log(K_{assoc}X_o)$ between -2.0 and 2.0. In the present case, $\log(K_{assoc}X_o) = \log[(327\ M^{-1})(1.09 \times 10^{-3}\ M)] = -0.45$. This value was approximated as -0.5 to facilitate the use of the working curve in Figure 11. From the resulting estimate of $\lambda^{1/2}K_{assoc}X_o = -0.46$ we obtain $k'_b = 7.4\ s^{-1}$. From analogous data at other scan rates in the kinetic regime we obtain $k'_b = 6.5\ s^{-1}$ at $\nu = 0.75$ V s^{-1} and $k'_b = 8.1\ s^{-1}$ at $\nu = 1$ V s^{-1}. An average of 7.3 s^{-1} is used in Table 2 for k'_b.

Acknowledgment. We thank the National Science Foundation for generous support of this research and acknowledge the helpful comments of a reviewer.

Supporting Information Available: A figure giving the cyclic voltammogram of $[Rh(COD)_2]^+$ in acetone in the presence of excess COD ($\nu = 0.2$ V s^{-1}). This material is available free of charge via the Internet at http://pubs.acs.org.

OM9900566